A New Model of Multiphonon Excitation Trap-Assisted Band-to-Band Tunneling

Juraj RACKO, Miroslav MIKOLÁŠEK, Alena GRMANOVÁ, Juraj BREZA, Peter BENKO, Ondrej GALLO, Ladislav HARMATHA

Faculty of Electrical Engineering and Information Technology, Slovak University of Technology, Ilkovičova 3, 812 19 Bratislava, Slovakia

juraj.racko@stuba.sk

Abstract. *The paper describes a new approach to calculating the currents in a pn-diode based on the extension of the Shockley-Read-Hall recombination-generation model. The presented theory is an alternative to Schenk's model of trap-assisted tunneling. The new approach takes into account generation and recombination as well as tunneling processes in pn-junctions. Using this model, the real "soft" I-V curve usually observed in the case of switching diodes and transistors was modeled as a result of the high concentration of traps that assist in the process of tunneling.*

Keywords

Shockley-Read-Hall model, Schenk model, trap assisted tunneling, *pn*-junction, *I-V* curve.

1. Introduction

Electrical characteristics of gate dielectric stacks strongly affect the reliability and non-volatility of memory devices. Leakage currents in these stacks are adversely influenced by defects present in the dielectrics that act as deep energy levels and bring about indirect, trap-assisted tunneling (TAT) of charge carriers. Under certain densities and distributions of the traps in the dielectrics, the TAT leakage current may assume dominant magnitudes.

In the last decade a number of models of TAT have been proposed [1 - 5]. In common, they allow to retrieve the energy levels and the densities of trapping centers by fitting the parameters of the models to experimentally obtained data. More recently, also a simple graphical method was developed for extraction of TAT parameters in thin n-Si/SiO_2 structures [6].

Attempts have been made to formulate compact unified models of TAT [7 - 9], nevertheless, some questions remain still open and new approaches to the issue can be expected.

Trap-assisted tunneling results in a reduction of the Shockley-Read-Hall (SRH) recombination lifetimes in the regions of strong electric fields [10, 11]. *I-V* characteristics of a reverse biased *pn*-junction are extremely sensitive to defect-assisted tunneling. The classical SRH model assumes that intermediate trap centers with concentration N_t lie on a discrete energy level E_t. In our model we assume that the discrete energy level E_t is broadened due to interactions of intermediate trap centers with multiphonon lattice vibrations, which gives rise to a band of multiphonon excitation traps.

2. Theory

In our model, the distribution function D_t^i of the density of traps (index *i* denotes a particular donor or acceptor band of traps) in the band gap satisfies the normalizing condition

$$N_{\mathrm{t}}^i = \int_{E_{\mathrm{V}}(x)}^{E_{\mathrm{C}}(x)} D_{\mathrm{t}}^i(x,\varepsilon)\,\mathrm{d}\varepsilon \tag{1}$$

where N_{t}^i are donor or acceptor trap concentrations, and

$$D_{\mathrm{t}}^i(x,\varepsilon) = \frac{N_t^i M^i(\varepsilon)}{\int_{E_{\mathrm{V}}}^{E_{\mathrm{C}}} M^i(\varepsilon)\mathrm{d}\varepsilon} . \tag{2}$$

Here, $M(\varepsilon)$ is the multiphonon non-radiative transition probability for electron and hole capture [10]

$$M^i(\varepsilon,x) = \frac{1}{\sqrt{2\pi}\varepsilon_r}\frac{(\theta \mp S)^2}{\left(\theta^2+z^2\right)^{\frac{1}{4}}}\times$$
$$\times\exp\left(\sqrt{z^2+\theta^2}-\theta\ln\left(\frac{\theta}{z}+\sqrt{1+\left(\frac{\theta}{z}\right)^2}\right)-S\left(2f_B+1\right)-\frac{\varepsilon_{\mathrm{t}}^i}{2kT}\right) \tag{3}$$

where S is the Huang-Rhys factor representing the electron-phonon coupling, $\hbar\omega_0$ is the effective phonon energy, $\varepsilon_r = S\ \hbar\omega_0$ is the lattice relaxation energy, $\theta = \varepsilon_{\mathrm{t}}^i/(\hbar\omega_0)$, $\varepsilon_{\mathrm{t}}^i = \left|\varepsilon - E_{\mathrm{C}}(x) + E_{\mathrm{t}}^i\right|$, f_{B} is the Bose distribution function $f_B = \left(\exp\left(\frac{\hbar\omega_0}{kT}\right)-1\right)^{-1}$ and $z = 2S\sqrt{f_B(1+f_B)}$. The sign inside the bracket in the nominator is negative for $\varepsilon > E_{\mathrm{C}}(x) - E_{\mathrm{t}}$ and positive for $\varepsilon < E_{\mathrm{C}}(x) - E_{\mathrm{t}}$.

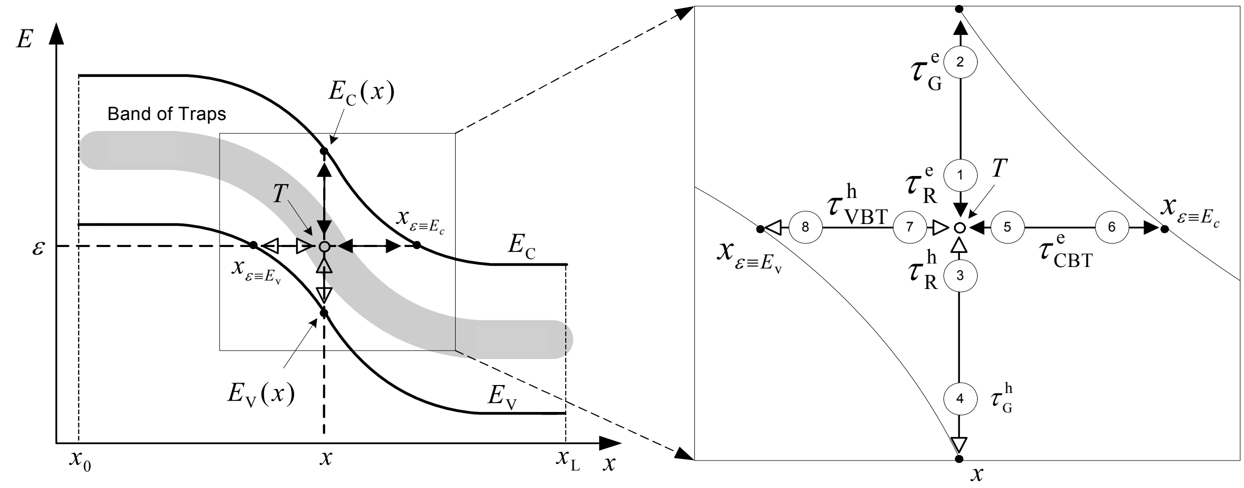

Fig. 1. Eight exchange processes considered in the new model of trap-assisted band-to-band tunnelling.

The current densities in the considered structures are calculated by solving the basic semiconductor laws, – the Poisson equation and continuity equation.

The continuity equations for electrons and holes can be written as

$$\frac{dJ^{e}_{D}(x)}{dx} = q\left(U_{SRH}(x)+U^{e(THER)}_{TAT}(x)+U^{e(TUN)}_{TAT}(x)\right), \quad (4)$$

$$\frac{dJ^{h}_{D}(x)}{dx} = -q\left(U_{SRH}(x)+U^{h(THER)}_{TAT}(x)+U^{h(TUN)}_{TAT}(x)\right) \quad (5)$$

where J^e_D, J^h_D are the drift-diffusion electron/hole current densities.

In our model of recombination we do not work with recombination lifetimes. Instead of them we introduce a set of the so-called escape times characterizing the exchange of electrons between the trap and the conduction or valence band. The physical model of the generation-recombination terms U_{SRH}, $U^{e(THER)}_{TAT}$, $U^{e(TUN)}_{TAT}$, $U^{h(THER)}_{TAT}$ and $U^{h(TUN)}_{TAT}$ taking into account the effect of trap-assisted tunneling is based on exchange processes of free charge carriers between the trap and the conduction or valence band (see Fig. 1). Four processes of electron and hole generation and recombination described by the classical SRH model are completed by four electron and hole capture and release processes of tunneling to and from the traps, giving together 8 exchange processes characterized by 6 escape times τ^e_R, τ^e_G, τ^h_R, τ^h_G, τ^e_{CBT} and τ^h_{VBT} [12 - 14]. From these 6 escape times one can derive the generation-recombination rates present in the continuity equations for electrons and holes.

2.1 Thermal Escape Times

1) Escape time $\tau^e_{R,i}$ describes the transition of the electron from position x in the CB (conduction band edge) to a trap lying at position x with a loss of electron energy (phonon transition)

$$\tau^e_{R,i}(x) = \frac{1}{v^e_{th}\sigma^i n(x)} \quad \text{where} \quad v^e_{th} = \sqrt{3kT/m^*_e} \quad (6, 7)$$

and σ^i is the trapping cross-section.

2) Escape time $\tau^e_{G,i}$ describes the transition of the electron from the trap lying at position x to CB at position x with an increase of electron energy (phonon transition)

$$\frac{1}{\tau^e_{G,i}(x,\varepsilon)} = \left(v^e_{th}\sigma^i N_C \exp\left(-\frac{E_c(x)-\varepsilon}{kT}\right)\right). \quad (8)$$

3) Escape time $\tau^h_{R,i}$ describes the transition of the hole from position x in the VB (valence band edge) to a trap lying at position x, with an increase of hole energy (phonon transition)

$$\tau^h_{R,i}(x) = \frac{1}{v^h_{th}\sigma^i p(x)} \quad \text{where} \quad v^h_{th} = \sqrt{3kT/m^*_h}\,. \quad (9)$$

4) Escape time $\tau^h_{G,i}$ describes the transition of the hole from the trap lying at position x to VB at position x with a loss of hole energy (phonon transition)

$$\frac{1}{\tau^h_{G,i}(x,\varepsilon)} = \left(v^h_{th}\sigma^i N_V \exp\left(-\frac{\varepsilon-E_V(x)}{kT}\right)\right). \quad (10)$$

2.2 Tunneling Escape Times

5) Escape time $\tau^e_{CBT,i}$ describes the transition of the electron from the cross-section $x_{\varepsilon\equiv E_C}$ lying in CB to the trap T lying at position x and in the opposite direction without any change in electron energy (tunnel transition)

$$\frac{1}{\tau^e_{CBT,i}(x,\varepsilon)} = \frac{m^e_R\sigma^i}{2\pi^2\hbar^3}\int_{E_C(x_L)}^{\varepsilon}\left|\varepsilon-\varepsilon'\right|\Gamma^e_{TAT}(\varepsilon', x_{\varepsilon\equiv E_C}-x)\,d\varepsilon' \quad (11)$$

where m^e_R is the effective mass for calculating the electron Richardson constant in the semiconductor and Γ^e_{TAT} is the probability of electron tunneling. In WKB approximation it is expressed as

$$\Gamma^{e}_{TAT}(\varepsilon, x_{\varepsilon\equiv E_C} - x) = \exp\left(-\frac{2}{\hbar}\int_{x_{\varepsilon\equiv E_C}}^{x}\sqrt{2m^{e}_{T}\left|E_C(x)-\varepsilon\right|}\,dx\right). \quad (12)$$

Here, m^{e}_{T} is the electron effective tunneling mass.

6) Escape time $\tau^{h}_{VBT,i}$ describes the transition of the hole from the cross-section $x_{\varepsilon\equiv E_V}$ lying in VB to trap T at position x and in the opposite direction without any change in hole energy (tunnel transition)

$$\frac{1}{\tau^{h}_{VBT,i}(x,\varepsilon)} = \frac{m^{h}_{R}\sigma^{i}}{2\pi^{2}\hbar^{3}}\int_{\varepsilon}^{E_V(x_L)}\left|\varepsilon-\varepsilon'\right|\Gamma^{h}_{TAT}(\varepsilon', x - x_{\varepsilon\equiv E_V})\,d\varepsilon' \quad (13)$$

where m^{h}_{R} is the effective mass for calculating the hole Richardson constant in the semiconductor and Γ^{h}_{TAT} is the probability of hole tunneling. In WKB approximation it is expressed as

$$\Gamma^{h}_{TAT}(\varepsilon, x - x_{\varepsilon\equiv E_V}) = \exp\left(-\frac{2}{\hbar}\int_{x_{\varepsilon\equiv E_V}}^{x}\sqrt{2m^{h}_{T}\left|E_V(x)-\varepsilon\right|}\,dx\right), \quad (14)$$

where m^{h}_{T} is the hole effective tunneling mass.

2.3 Generation-Recombination Terms

After computing the density of traps $D^{i}_{t}(x,\varepsilon)$ and single escape times we can evaluate the generation-recombination terms occurring in (4) and (5). The generation-recombination terms are expressed in (17) to (21), where f_{F_n} and f_{F_p} are the Fermi-Dirac distribution function for electrons and holes defined as

$$f_{F_n}(x_{\varepsilon\equiv E_C}) = 1\Bigg/\left(1+\exp\left(-\frac{\varepsilon - E_{F_n}(x_{\varepsilon\equiv E_C})}{kT}\right)\right). \quad (15)$$

and

$$f_{F_p}(x_{\varepsilon\equiv E_V}) = 1\Bigg/\left(1+\exp\left(-\frac{E_{F_p}(x_{\varepsilon\equiv E_V}) - \varepsilon}{kT}\right)\right). \quad (16)$$

Parameter $E_{F_n}(x_{\varepsilon=E_C})$ in (15) denotes the Fermi quasi-level for electrons at cross-section $x_{\varepsilon\equiv E_C}$ and $E_{F_p}(x_{\varepsilon=E_V})$ in (16) denotes the Fermi quasi-level for holes at cross-section $x_{\varepsilon=E_V}$, see Fig. 1. In (20) and (21),

$$F_C = \frac{dE_C(x_{\varepsilon\equiv E_c})}{dx} \text{ and } F_V = \frac{dE_V(x_{\varepsilon\equiv E_v})}{dx}$$

are the electron and hole driving forces, respectively.

3. Results of Simulation

The new TAT model was employed in simulations of a pn-diode with a linear concentration profile (Fig. 2) prepared on a phosphorous doped silicon substrate (N_D=2.5×10^{18} cm^{-3}) with orientation <111> by boron diffusion from an infinite source with surface concentration N_A=10^{19} cm^{-3} at a temperature of 1020°C for 30 minutes. The structure was contaminated by gold, which forms one acceptor band of traps (i=A) at a distance of E_t^A=0.54 eV from the conduction band edge. The concentration of the atoms of gold was assumed to be N_t^A=10^{14} cm^{-3}. The effective cross section was set for electrons and holes constant σ^A=10^{-15} cm^2. For evaluating the tunneling escape times τ^{e}_{CBT}, effective masses m_R^e=2.19 m_0 and for τ^{h}_{VBT}, m_R^h=0.66 m_0 were used [15]. The tunneling probability was calculated using the WKB approximation and the effective masses were set as m_T^e=0.26 m_0 and m_T^h=0.37 m_0.

Fig. 3 shows the simulated reverse *I-V* curve. For comparing the influence of TAT mechanisms the *I-V* curve calculated only with the SRH model is depicted as well. Trap-assisted-tunneling results in an increase of the current in the middle voltage region, resulting to a "soft" shape of the *I-V* curve. At higher voltages, however, the influence of TAT mechanisms becomes negligible in comparison with band-to-band processes.

Fig. 4 displays *I-V* characteristics with a constant Huang-Rhys factor S=4, for different effective energies $\hbar\omega_0$=12, 24, 36, 48 and 60 meV. The change of $\hbar\omega_0$ affects both the normalized distribution function $D^A(\hbar\omega_0)$ and the normalizing integral $\int_{E_V}^{E_C} M^{A}(\varepsilon)d\varepsilon$, thus the denominator in (2), see Figs. 5 and 6. This eventually affects the multiphonon broadening of the deep trap level. A decrease in the multiphonon effective energy has a dramatic impact upon the growth of the current density even if the density of traps N_t in the band remains unchanged.

Fig. 7 shows the reverse *I-V* curves with a constant multiphonon effective energy $\hbar\omega_0$= 24 meV for different values of the Huang-Rhys factor, S=2, 4, 6, 8 and 10. Similarly like the effective energy $\hbar\omega_0$, the Huang-Rhys factor has an influence on the broadening of the band of traps. In Figs. 8 and 9 one can see how the Huang-Rhys factor affects the distribution function $D^A(S)$ and the normalization integral.

4. Conclusion

It is obvious that multiphonon broadening of the band of traps and trap-assisted tunneling markedly affect the reverse currents in heavily doped pn-junctions. Our simulations reveal that the effective energy $\hbar\omega_0$ has a slightly stronger effect on the current than the Huang-Rhys factor. The new TAT model has the ability to describe the generation and recombination as well as the tunneling processes in pn-junctions. Using this model, the real "soft" *I-V* curve usually observed in the case of switching diodes and transistors was modeled as a result of the high concentration of traps that assist in the process of tunneling.

$$U_{\mathrm{SRH}}(x)=\sum_{i=\mathrm{D,A}}\int_{E_{\mathrm{V}}(x)}^{E_{\mathrm{C}}(x)}\frac{\left(\frac{1}{\tau^{\mathrm{e}}_{\mathrm{R},i}(x)}\frac{1}{\tau^{\mathrm{h}}_{\mathrm{R},i}(x)}-\frac{1}{\tau^{\mathrm{e}}_{\mathrm{G},i}(x,\varepsilon)}\frac{1}{\tau^{\mathrm{h}}_{\mathrm{G},i}(x,\varepsilon)}\right)D^{i}_{\mathrm{t}}(x,\varepsilon)\mathrm{d}\varepsilon}{\frac{1}{\tau^{\mathrm{e}}_{\mathrm{R},i}(x)}+\frac{1}{\tau^{\mathrm{e}}_{\mathrm{G},i}(x,\varepsilon)}+\frac{1}{\tau^{\mathrm{h}}_{\mathrm{R},i}(x)}+\frac{1}{\tau^{\mathrm{h}}_{\mathrm{G},i}(x,\varepsilon)}+\frac{1}{\tau^{\mathrm{e}}_{\mathrm{CBT},i}(x,\varepsilon)}+\frac{1}{\tau^{\mathrm{h}}_{\mathrm{VBT},i}(x,\varepsilon)}}\tag{17}$$

$$U^{\mathrm{e(THER)}}_{\mathrm{TAT}}(x)=$$

$$=\sum_{i=\mathrm{D,A}}\int_{E_{\mathrm{V}}(x)}^{E_{\mathrm{C}}(x)}\frac{\frac{1}{\tau^{\mathrm{e}}_{\mathrm{R},i}}\left(\frac{1-f_{\mathrm{F_n}}(x_{\varepsilon\equiv E_{\mathrm{C}}})}{\tau^{\mathrm{e}}_{\mathrm{CBT},i}}+\frac{f_{\mathrm{F_p}}(x_{\varepsilon\equiv E_{\mathrm{V}}})}{\tau^{\mathrm{h}}_{\mathrm{VBT},i}}\right)-\frac{1}{\tau^{\mathrm{e}}_{\mathrm{G},i}}\left(\frac{f_{\mathrm{F_n}}(x_{\varepsilon\equiv E_{\mathrm{C}}})}{\tau^{\mathrm{e}}_{\mathrm{CBT},i}}+\frac{1-f_{\mathrm{F_p}}(x_{\varepsilon\equiv E_{\mathrm{V}}})}{\tau^{\mathrm{h}}_{\mathrm{VBT},i}}\right)}{\frac{1}{\tau^{\mathrm{e}}_{\mathrm{R},i}}+\frac{1}{\tau^{\mathrm{e}}_{\mathrm{G},i}}+\frac{1}{\tau^{\mathrm{h}}_{\mathrm{G},i}}+\frac{1}{\tau^{\mathrm{h}}_{\mathrm{R},i}}+\frac{1}{\tau^{\mathrm{e}}_{\mathrm{CBT},i}}+\frac{1}{\tau^{\mathrm{h}}_{\mathrm{VBT},i}}}D^{i}_{\mathrm{t}}\mathrm{d}\varepsilon\tag{18}$$

$$U^{\mathrm{h(THER)}}_{\mathrm{TAT}}(x)=$$

$$=\sum_{i=\mathrm{D,A}}\int_{E_{\mathrm{V}}(x)}^{E_{\mathrm{C}}(x)}\frac{\frac{1}{\tau^{\mathrm{h}}_{\mathrm{R},i}}\left(\frac{f_{\mathrm{F_n}}(x_{\varepsilon\equiv E_{\mathrm{C}}})}{\tau^{\mathrm{e}}_{\mathrm{CBT},i}}+\frac{1-f_{\mathrm{F_p}}(x_{\varepsilon\equiv E_{\mathrm{V}}})}{\tau^{\mathrm{h}}_{\mathrm{VBT},i}}\right)-\frac{1}{\tau^{\mathrm{h}}_{\mathrm{G},i}}\left(\frac{1-f_{\mathrm{F_n}}(x_{\varepsilon\equiv E_{\mathrm{C}}})}{\tau^{\mathrm{e}}_{\mathrm{CBT},i}}+\frac{f_{\mathrm{F_p}}(x_{\varepsilon\equiv E_{\mathrm{V}}})}{\tau^{\mathrm{h}}_{\mathrm{VBT},i}}\right)}{\frac{1}{\tau^{\mathrm{e}}_{\mathrm{R},i}}+\frac{1}{\tau^{\mathrm{e}}_{\mathrm{G},i}}+\frac{1}{\tau^{\mathrm{h}}_{\mathrm{G},i}}+\frac{1}{\tau^{\mathrm{h}}_{\mathrm{R},i}}+\frac{1}{\tau^{\mathrm{e}}_{\mathrm{CBT},i}}+\frac{1}{\tau^{\mathrm{h}}_{\mathrm{VBT},i}}}D^{i}_{\mathrm{t}}\mathrm{d}\varepsilon\tag{19}$$

$$U^{\mathrm{e(TUN)}}_{\mathrm{TAT}}(x_{\varepsilon\equiv E_{\mathrm{c}}})=$$

$$\sum_{i=\mathrm{D,A}}\left|F_{\mathrm{C}}\right|\int_{x_{\varepsilon\equiv E_{\mathrm{V}}}}^{x_{\varepsilon\equiv E_{\mathrm{C}}}}\frac{\frac{f_{\mathrm{F_n}}(x_{\varepsilon\equiv E_{\mathrm{C}}})}{\tau^{\mathrm{e}}_{\mathrm{CBT},i}}\left(\frac{1}{\tau^{\mathrm{e}}_{\mathrm{G},i}}+\frac{1}{\tau^{\mathrm{h}}_{\mathrm{R},i}}+\frac{1}{\tau^{\mathrm{h}}_{\mathrm{VBT},i}}\right)-\frac{1-f_{\mathrm{F_n}}(x_{\varepsilon\equiv E_{\mathrm{C}}})}{\tau^{\mathrm{e}}_{\mathrm{CBT},i}}\left(\frac{1}{\tau^{\mathrm{e}}_{\mathrm{R},i}}+\frac{1}{\tau^{\mathrm{h}}_{\mathrm{G},i}}+\frac{1}{\tau^{\mathrm{h}}_{\mathrm{VBT},i}}\left(\frac{1-f_{\mathrm{F_p}}(x_{\varepsilon\equiv E_{\mathrm{V}}})}{1-f_{\mathrm{F_n}}(x_{\varepsilon\equiv E_{\mathrm{C}}})}\right)\right)}{\frac{1}{\tau^{\mathrm{e}}_{\mathrm{R},i}}+\frac{1}{\tau^{\mathrm{e}}_{\mathrm{G},i}}+\frac{1}{\tau^{\mathrm{h}}_{\mathrm{G},i}}+\frac{1}{\tau^{\mathrm{h}}_{\mathrm{R},i}}+\frac{1}{\tau^{\mathrm{e}}_{\mathrm{CBT},i}}+\frac{1}{\tau^{\mathrm{h}}_{\mathrm{VBT},i}}}D^{i}_{\mathrm{t}}\mathrm{d}x\tag{20}$$

$$U^{\mathrm{h(TUN)}}_{\mathrm{TAT}}(x_{\varepsilon\equiv E_{\mathrm{V}}})=$$

$$=\sum_{i=\mathrm{D,A}}\left|F_{\mathrm{V}}\right|\int_{x_{\varepsilon\equiv E_{\mathrm{V}}}}^{x_{\varepsilon\equiv E_{\mathrm{C}}}}\frac{\frac{f_{\mathrm{F_p}}(x_{\varepsilon\equiv E_{\mathrm{V}}})}{\tau^{\mathrm{h}}_{\mathrm{VBT},i}}\left(\frac{1}{\tau^{\mathrm{e}}_{\mathrm{R},i}}+\frac{1}{\tau^{\mathrm{h}}_{\mathrm{G},i}}+\frac{1}{\tau^{\mathrm{e}}_{\mathrm{CBT},i}}\frac{f_{\mathrm{F_n}}(x_{\varepsilon\equiv E_{\mathrm{C}}})}{f_{\mathrm{F_p}}}\right)-\frac{1-f_{\mathrm{F_p}}(x_{\varepsilon\equiv E_{\mathrm{V}}})}{\tau^{\mathrm{h}}_{\mathrm{VBT},i}}\left(\frac{1}{\tau^{\mathrm{e}}_{\mathrm{G},i}}+\frac{1}{\tau^{\mathrm{h}}_{\mathrm{R},i}}+\frac{1}{\tau^{\mathrm{e}}_{\mathrm{CBT},i}}\right)}{\frac{1}{\tau^{\mathrm{e}}_{\mathrm{R},i}}+\frac{1}{\tau^{\mathrm{e}}_{\mathrm{G},i}}+\frac{1}{\tau^{\mathrm{h}}_{\mathrm{G},i}}+\frac{1}{\tau^{\mathrm{h}}_{\mathrm{R},i}}+\frac{1}{\tau^{\mathrm{e}}_{\mathrm{CBT},i}}+\frac{1}{\tau^{\mathrm{h}}_{\mathrm{VBT},i}}}D^{i}_{\mathrm{t}}\mathrm{d}x\tag{21}$$

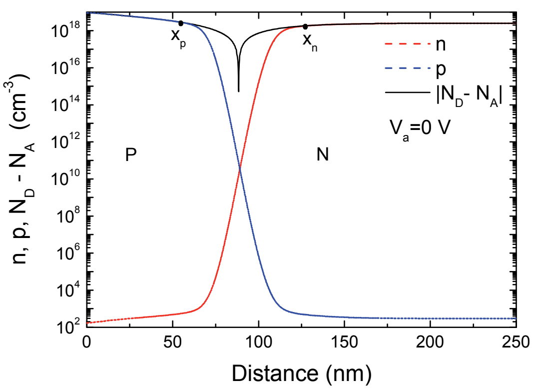

Fig. 2. Concentration profile of the simulated *pn*-diode.

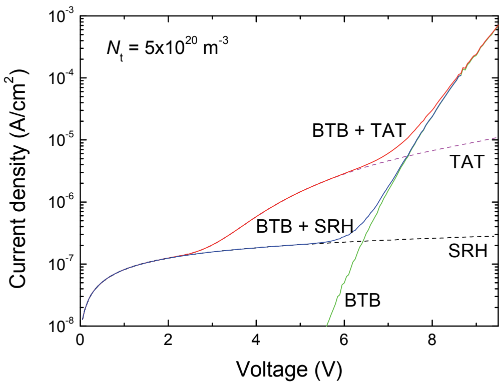

Fig. 3. Comparison of our TAT model with classical SRH model.

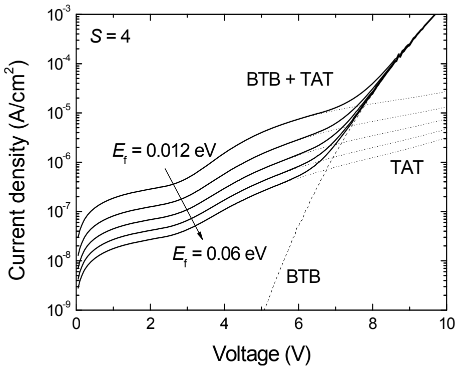

Fig. 4. Reverse *I-V* characteristics for a constant Huang-Rhys factor *S*=4*,* for different effective energies $\hbar\omega_0$=12, 24, 36, 48 and 60 meV.

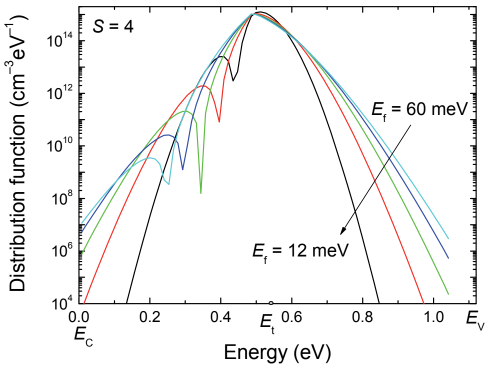

Fig. 5. The distribution function in dependence on the effective energy $\hbar\omega_0 \equiv E_f$.

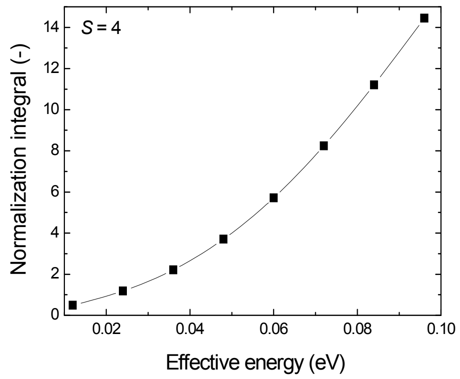

Fig. 6. Normalization integral for different effective energies $\hbar\omega_0$=12, 24, 36, 48 and 60 meV and constant Huang-Rhys factor *S*=4.

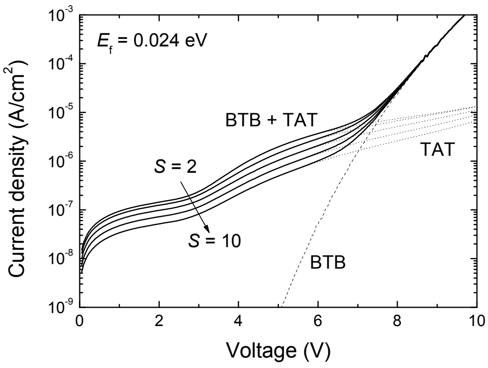

Fig. 7. Reverse *I-V* characteristics curves for a constant multiphonon effective energy $\hbar\omega_0$=24 meV, for different values of the Huang-Rhys factor, *S*=2, 4, 6, 8 and 10.

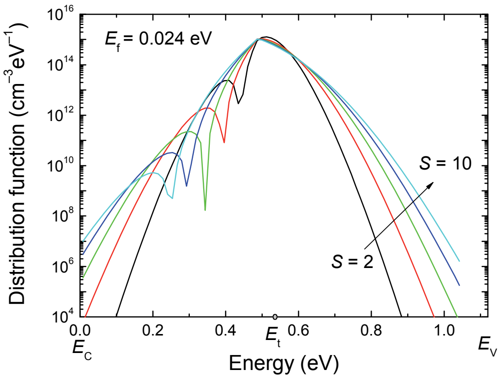

Fig. 8. The distribution t function for different values of the Huang-Rhys factor, *S*=2, 4, 6, 8 and 10.

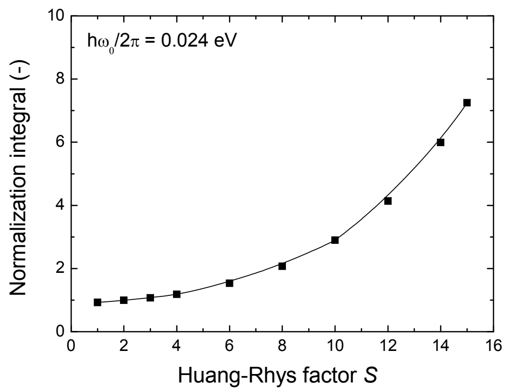

Fig. 9. Normalization integral for different values of the Huang-Rhys factor *S*=2, 4, 6, 8 and 10, and constant $\hbar\omega_0$=24 meV.

Acknowledgement

The work has been conducted at the Institute of Electronics and Photonics, FEI STU in Bratislava, in the Centre of Excellence CENAMOST (VVCE-0049-07), and supported by the Slovak Research and Development Agency (projects APVV-0509-10) and by the Scientific Grant Agency of the Ministry of Education of the Slovak Republic (projects VEGA 1/0712/12).

References

[1] HOUSSA, M., TUOMINEN, M., NAILI, M., AFANASEV, A., HAUKKA, S., HEYNS, M. M. Trap-assisted tunneling in high permittivity gate dielectric stacks. *Journal of Applied Physics*, 2000, vol. 87, no. 12, p. 71 - 73.

[2] HOUSSA, M., STESMANS, A., HEYNS, M. M. Model for the trap-assisted tunneling current through very thin SiO_2/ZrO_2 gate dielectric stacks. *Semiconductor Science and Technology*, 2001, vol. 16, no. 6, p. 427 – 432.

[3] IELMINI, D., SPINELLI, A. S., LACAITA, A. L., MARTINELLI, A., GHIDINI, G. A recombination- and trap-assisted tunneling model for stress-induced leakage current. *Solid-State Electronics*, 2001, vol. 45, no. 8, p. 1361 – 1369.

[4] JIMÉNEZ-MOLINOS, F., PALMA, A., GÁMIZ, F., BANQUERI, J., LÓPEZ-VILLANUEVA, J. A. Physical model for trap-assisted inelastic tunneling in metal-oxide-semiconductor structures. *Journal of Applied Physics*, 2001, vol. 90, no. 7, p. 3396 – 3404.

[5] JIMÉNEZ-MOLINOS, F., GÁMIZ, F., PALMA, A., CARTUJO, P., LÓPEZ-VILLANUEVA, J. A. Direct and trap-assisted tunneling through ultrathin gate oxides. *Journal of Applied Physics*, 2002, vol. 91, no. 8, p. 5116 - 5124.

[6] GUSHTEROV, A., SIMEONOV, S. Extraction of trap-assisted tunneling parameters by graphical method in thin n-Si/SiO_2 structures. *Journal of Optoelectronics and Advanced Materials*, 2005, vol. 7, no. 3, p. 1389 – 1393.

[7] SATHAIYA, D. M., KARMALKAR, S. A closed-for model for thermionic trap-assisted tunneling. *IEEE Transactions on Electron Devices*, 2008, vol. 55, no. 2, p. 557 - 564.

[8] RANA, A. K., CHAND, N., KAPOOR, V. Trap assisted tunneling model for gate current in nano scale MOSFET with high-K dielectrics. *International Journal of Electrical and Electronics Engineering*, 2009, vol. 3, no. 7, p. 400 - 407.

[9] ZHANG, M., HUO, Z., YU, Z., LIU, J., LIU, M. Unification of three multiphonon trap-assisted tunneling mechanisms. *Journal of Applied Physics*, 2011, vol. 110, no. 11, p. 1.3662195 (11 pages).

[10] SCHENK, A. A model for the field and temperature dependence of Shockley-Read-Hall lifetimes in silicon. *Solid-State Electronics*, 1992, vol. 35, no. 11, p. 1585 - 1596.

[11] HURKX, G.A.M., KLAASSEN, D.B.M., KNUVERS, M.P.G. A new recombination model for device simulation including tunneling. *IEEE Transactions on Electron Devices*, 1992, vol. 39, no. 2, p. 331 – 338.

[12] MIKOLÁŠEK, M., RACKO, J., HARMATHA, L., GALLO, O., REŽNÁK, J., SCHWIERZ, F., GRANZNER, R. A new model of trap assisted band-to-band tunnelling. In *Proceedings of the 8th International Conference on Advanced Semiconductor Devices and Microsystems ASDAM'10*. Smolenice Castle (Slovakia), 2010, p. 195 - 198.

[13] RACKO, J., MIKOLÁŠEK, M., GRANZNER, R., BREZA, J., DONOVAL, D., GRMANOVÁ, A., HARMATHA, L., SCHWIERZ, F., FRÖHLICH, K. Trap-assisted tunnelling current in MIM structures. *Central European Journal of Physics*, 2011, vol. 9, no. 1, p. 230 - 241.

[14] RACKO, J., MIKOLÁŠEK, M., HARMATHA, L., BREZA, J., HUDEC, B., FRÖHLICH, K., AARIK, J., TARRE, A., GRANZNER, R., SCHWIERZ, F. Analysis of leakage current mechanisms in RuO_2-TiO_2-RuO_2 MIM structures. *Journal of Vacuum Science and Technology B*, 2011, vol. 29, no. 1, p. 01AC08-1 - 01AC08-8.

[15] SZE, S. M. *Physics of Semiconductor Devices*. 2nd ed. New York, Chichester, Brisbane, Toronto, Singapore: John Wiley & Sons, 1981 (page 257).

About Authors

Juraj RACKO (PhD) was born in 1953. His research interests include modeling and simulation of semiconductor structures and devices.

Miroslav MIKOLÁŠEK was born in 1983. Currently he is a PhD student. His interests include modeling and simulation of semiconductor structures and devices.

Alena GRMANOVÁ (RNDr) is a research worker involved in materials technology.

Juraj BREZA (Prof) was born in 1951. His teaching and research activities are focused on thin films and materials analysis.

Peter BENKO (PhD) was born in 1981. Currently he is a research worker active mainly in device simulation.

Ondrej GALLO was born in 1981. His research is focused on synthesis of digital circuits with using Petri nets.

Ladislav HARMATHA (Assoc Prof) was born in 1948. His current activities are focused on semiconductor structures.